Egypt. J. Chem. **Vol. 66,** No. 12, pp. 511 - 527 (2023)

Egyptian Journal of Chemistry

http://ejchem.journals.ekb.eg/

Profiling the volatile composition and cytotoxic assessment of the encapsulated *Spirulina Platensis* using alginate chitosan nanoparticles

Warda M. Fadl Allah [a*], Mohamed Abbas Shemis [a], Eman M. Abd El Azeem [b], Ezzat E. A. Osman [c], Samah Mamdouh [a]

[a] *Department of Biochemistry and Molecular Biology, Theodor Bilharz Research Institute, Kornaish El-Nile St., 12411, Giza, Egypt.*

[b] *Department of Medicinal Chemistry, Theodor Bilharz Research Institute, Kornaish El-Nile St., 12411, Giza, Egypt.*

[c] Department of Biochemistry, Faculty of Science, Ain Shams University, Cairo, Egypt.

Abstract

Spirulina platensis (S. platensis) is a blue-green microalga that belongs to the cyanobacteria family. The goal of this research was to investigate the anticancer activity of encapsulation *S. platensis* algae with Chitosan-Alginate polyelectrolyte nanoparticles on HepG-2, Caco-2, and Vero cell lines and profile its chemical components. *S.platensis* was extracted using 90% MeOH as a crude extract which was fractionated using different organic solvents. While Nanoencapsulation of 90% MeOH ext. and pet-ether fr. by Chitosan-Alginate polyelectrolyte nanoparticles were prepared by modified ionic gelation method. The chemical composition of 90% MeOH ext. was identified using the GC-MS technique. The 90% MeOH ext. of *S. platensis* showed high toxicity on HepG-2 and Caco-2 cells, more than the pet-ether fraction. While they were safe on Vero normal cells. Furthermore, nanoencapsulation of the 90%MeOH ext. and pet-ether fr. increased the cytotoxicity against HepG-2 and Caco-2 cells. Moreover, The effect of 90%MeOH ext. and pet-ether fr. NPs against HepG-2 and Caco-2 resulted in a significant increase in the relative expression of the Caspase-3 enzyme and a decrease in the expression of the TNF-α gene and COX-2 enzyme more than the non-encapsulated form. The GC-MS analysis of the silylated 90 % MeOH ext. revealed the presence of 57 bioactive compounds including, alcohols, terpenes, organic acids, and others.

Keywords: anti-cancer, *Spirulina platensis*, Alginate, nanoencapsulation, GC-MS analysis.

1. Introduction

Millions of people worldwide die from cancer each year [1], making it one of the most deadly diseases in existence today. It is one of the most important modern health issues because it knows no boundaries and can affect any organ. The World Health Organization (WHO) estimates that cancer will be the major cause of roughly 10 million deaths worldwide in 2020 [2]. Cancer caused nearly 1 out of every 6 fatalities, yet it is ranked as the second leading cause of death worldwide [3]. When the balance between cell growth and cell death was off, cancer began to occur in multicellular organs. The majority of anticancer medications created to treat cancer have been demonstrated to cause cancer cells to undergo apoptosis. The endonucleolytic breakage of DNA and alterations in chromatin condensation of cancer cells caused by those anticancer medicines also cause apoptotic cell death [4]. Chemopreventive drugs for cancer use natural, synthetic, or biological chemicals to halt, delay, or prevent the transformation of neoplastic cells into cancer or the initiation of the carcinogenesis process. Much prior research has demonstrated that cyclooxygenase 2 (COX-2) inhibitors are advantageous in reducing the incidence of skin, liver, and colon cancer and function effectively as chemo-preventive medicines [5]. Although there are various treatments available, persistent resistance to these treatments focuses on the need for innovative cancer control alternatives[6]. The development of a new generation of anticancer medications now being tested in clinical trials is the result of technological improvements and significant research on marine natural ingredients [7].

Recently, the blue-green microalga *Spirulina platensis (S. platensis)* has attracted attention due to its potential to be exploited as a source of bioactivities with therapeutic advantages that may be used in medicine, including the treatment of cancer [8].

*Corresponding author e-mail: wardamohamed2111@gmail.com.; (Warda M. Fadl Allah).

Receive Date: 11 March 2023, Revise Date: 29 March 2023, Accept Date: 21 May 2023, First Publish Date: 21 May 2023

DOI: 10.21608/ejchem.2023.199387.7718

The free-floating blue-green microalga *Spirulina platensis*, which is a member of the cyanobacteria family and has outstanding anti-oxidative capabilities, has been the subject of most research [9]. It is considered a promising healthy food due to its high protein content (60-70% by dry weight) reaching five times that of meat and can provide the majority of essential amino acids. Also, its richness in polysaccharides (15-20%), minerals, vitamins (B12 & E), essential fatty acids, carotenoids, carbohydrates, zeaxanthin, myxo xanthophyll, and phycocyanin [10,11,12]. These main constituents make it promising for the food industry to overcome the problem of malnutrition and in health applications against pathogens[13] Moreover, *S. platensis* is frequently employed in conventional medicine to prevent and treat several chronic illnesses, including cancer, obesity, arterial hypertension, toxicity brought on by heavy metals and chemicals, radiation damage, anemia, and dyslipidemia[13].

At present, the prominence of algal biotechnology is rapidly developing and increasing. Since the first studies, different species have been discovered and algae have become the focal point of new research in a Short time with the evaluation of materials obtained from these species [14].

With a great impact on numerous biomedical sectors, nanomaterials are increasingly being utilized in innovative products as biosensors and drug delivery systems [15]. Polymeric nanoparticles may offer tailored drug delivery, which is particularly useful for cancer therapy and significantly reduces the systemic adverse effects of extremely toxic anticancer medications. Moreover, poorly water-soluble medicines may benefit from the sustained release offered by polymer-based nano-carriers and increase their bioavailability[16]. To preserve their positive benefits, encapsulating algal bio-active components has become urgently necessary. Alginates, one of the most significant algae bio-actives, are being employed more and more in applications like biomaterials for tissue engineering and bio-printing [17]. Although alginates are typically utilized in industry for their physical qualities such as stabilizing, thickening, and emulsifying properties, they can also be employed for specialized attributes such as gel strength, porosity, or biocompatibility [18].

Researchers have created nanoparticles throughout the last few decades using lipids, polysaccharides, lipid-derived biopolymers, synthetic biodegradable polymers, and natural biopolymers. The idea of delivering medicine via nanoparticles made of natural biodegradable polymers has recently attracted a lot of attention. Alginate and chitosan are two of these and have been widely employed in the pharmaceutical industry for controlling medicine release [19].

Chitosan and Alginate polysaccharides are used as natural biomaterials, as they are highly stable, safe, non-toxic, hydrophilic, and bio-degradable [20].

The overall goal of this research was to investigate the anticancer activity of *Spirulina platensis* extracts and their derivative fractions on HepG-2, Caco-2, and Vero cell lines and profile its chemical components.

Experimental:

Algae materials and chemicals for extraction and fractionation.

Spirulina platensis algae powder was obtained from National Research Center (N.R.C), Giza, Egypt, from professor Mohamed Hassoub, it was collected from freshwater, Red sea, Hurghada. At the beginning of 2020 exactly in February. Methanol (MeOH), Ethyl acetate (EtOAc), Petroleum ether 60°-80°C (pet-ether) and n-Butanol (BuOH) all solvents were purchased from El- Gomhoria Company, Egypt.

1. xtraction and Fractionation Process:

One hundred grams of *S. platensis* dried powder material was extracted using 90 % MeOH, and then evaporated under reduced pressure using a rotatory evaporator (BUCHI, Switzerland) under vacuum till dryness to get 30.8 g of MeOH ext. After dryness, 28 g of dried 90%MeOH ext. were dissolved in less amount of distilled water, then fractionated using organic solvents including pet-ether 60° -80°C, EtOAc, and BuOH. Each fraction was dried using a rotatory evaporator and the water residue was completely dried to get 3.2 g of pet-ether fr., 2.0 g of EtOAc, 4.8 g of BuOH fr., and 18.5 g of water fraction. The crude 90% MeOH ext. and its derivative fractions were stored in air-tight containers under dark cold conditions until further analysis [21].

2. Cell Lines and Cell Culture:

Colon (Caco-2), liver (HepG-2) cancer cell lines and normal Vero cells were obtained from the regional center for mycology and biotechnology (Al-Azhar University, Cairo, Egypt). The RPMI 1640 w /stable Glutamine (Thermo Fisher Scientific, USA) was used for cancerous cell lines culture and Dulbecco's Modified Eagle Medium (DMEM) (Thermo Fisher Scientific, USA) was used for normal cell line culture. The cells were cultured in a specific growth media (GM) supplemented with 10% inactivated fetal bovine serum (FBS), 1% antibiotic (penicillin/streptomycin) fungizone solution

(LONZA), incubated in humidified, 5% CO2 atmosphere at 37 °C.

3. In-vitro Assays for Cytotoxic Activity:

The anticancer activity of the 90%MeOH ext. of *S. platensis* algae was analyzed using two cancerous cell lines Caco-2, HepG-2, and normal cell line Vero. Cells were cultured in a specific GM and then incubated at 37°C and 5% CO2 until the cells made a complete sheet. Cells were treated with different concentrations (6.25, 12.5, 25, 50, 100, and 200 µg/mL) of 90%MeOH ext., and its derivative fractions with untreated cells serving as control were used and the plate was incubated for 72 hrs at 37°C, the cell sheet was washed three times with phosphate buffer saline (PBS), then 10 µl of 5 mg/ml MTT (3-(4,5-dimethylthiazol-2-yl)-2,5-diphenyltetrazolium bromide) reagent was added to each well and incubated for another 4 hrs in the dark.

The supernatant was removed, and 200 µl of dimethyl sulfoxide (DMSO) was added to each well including control, followed by shaking, and then the plate was kept in a dark place at room temperature for about 10 min. Absorbance was measured at 490 nm using an ELISA reader (PerkinElmer, Waltham, MA). The efficiency of 90%MeOH ext. and the four fractions was calculated according to the following equation:

Cell viability % = (absorbance of treated cells/absorbance of cell control) x 100 [22].

All experiments were performed in triplicate and mean values were used for calculation.

4. Preparation of *S. platensis* Loaded Chitosan-Alginate Nanoparticles:

Encapsulation of *S. platensis* algae extract and fractions by CS-ALG NPs was performed to enhance the activity, targeting and decreasing the side effects.

4.1. Reagents and chemicals used for Encapsulation:

Low-viscosity sodium alginate, chitosan, low molecular weight, deacetylated CS poly (D-glucosamine), and glacial acetic acid, were obtained from Sigma-Aldrich (USA). PBS, sodium hydroxide, tween 80, and hydrochloric acid were supplied by (Loba chemical, India). All other reagents were of analytical grade and ultrapure water with a resistivity of 18 µS/cm was obtained from an ultrapure water system (Millipore Milli-Q system; Milford, MA, USA) and used in all aqueous preparations.

4.2. Preparation of Chitosan-Alginate polyelectrolyte Nanoparticles:

Both *S. platensis* 90%MeOH ext. and pet-ether fr. CS-ALG NPs as well as CS-ALG empty NPs were prepared by a slightly modified ionic gelation method. The chitosan powder was dissolved in 40 mL of acetic acid (1% v/v) to a concentration of 2 mg/ mL and adjusted to pH 5.5, 1mg/mL of the alginate solution was prepared by dissolving 20 mg of the alginate powder in 20 mL distilled water at room temperature for overnight. For the *S. platensis* loaded NPs, 50 mg of each extract was stirred with 20 mL alginate solution for 24 hrs to form the *S. platensis* alginate complex. Also, 40 mL of the chitosan solution was stirred with 0.310 g of tween 80 at 60°C for 2 hrs to obtain a homogeneous mixture and this solution was gradually dropped to the *S. platensis* alginate complex for 1 hr during stirring at a high speed. The stirring was continued for another 20 min to ensure the complete formation of the NPs which were then refrigerated overnight. CS-ALG empty NPs were prepared as a negative control. NPs suspension was centrifuged at 12000 rpm for 30 min to obtain NPs pellets and the supernatant was collected for determining the percentage of encapsulation efficiency and the loading capacity. The resuspended pellet was frozen overnight at −80°C and subsequently, transferred to the freeze dryer under the standard conditions of 7 bars pressure, inlet temperature was 96°C, and the achieved outlet temperature was 65° -70°C [23].

5. Characterization of *S. platensis* Loaded Nanoparticle:

5.1. Structural Analysis of Nanoparticles:

The morphology and the structural features size of the prepared 90% MeOH ext., NPs, and pet-ether fr. NPs were analyzed using a transmission electron microscope (TEM) (Leo 0430, Leica, Cambridge, UK), and the surface charge (zeta potential) of NPs was compatible with TEM analysis. TEM samples were prepared as follows, about 1 mg of *S. platensis* NP was dissolved in 1 mL distilled water, the sample was sonicated at 37°C for 20 minutes to get a dispersed suspension, a small drop of the particle suspension was placed onto a carbon-coated copper grid and dried completely before observation, about 2 minutes after deposition, the grid was tapped with a filter paper to remove any excess water, and finally images were taken using a transmission electron microscope.

5.2. FTIR Analysis:

The Fourier transform infrared (FTIR) spectra of CS-ALG unloaded NPs, and *S. platensis* extracts loaded NPs were obtained using Bruker VERTEX 80 (Germany), supplied with a diamond disk as that of an internal reflector in the range 4000-400 cm-1 with resolution 4 cm-1, and reflective index 2.4.

6. Determination of the encapsulation efficiency and the drug loading percentages of Chitosan-Alginate *S. platensis* nanoparticles:

The amount of the incorporated *S. platensis* in the CS-ALG NPs was determined by measuring the absorbance of *S. platensis* remaining in the supernatant (free *S. platensis*) after centrifugation of the NPs mixture. A calibration curve was performed with a series of concentrations to obtain the unknown *S. platensis* concentrations by using Nano-Drop®2000c Spectrophotometer (Thermo Scientific, USA) at wavelength 620 nm.

The percent encapsulation efficiency **(% EE)** was calculated as follows;

(Eq. 1) % EE = *S. platensis* 0 − *S. platensis* F / *S. platensis 0* × 100.

Where *S. platensis* 0 is the initial amount of *S. platensis* added for encapsulation and *S. platensis* F is the amount of non-entrapped *S. platensis* in the supernatant after centrifugation of the particles [24].

Also, the loading capacity of *S. platensis* onto the CS-ALG particles was determined according to the equation:

(Eq. 2) Loading capacity = (*S. platensis* 0 – *S. platensis* F)/ NPs wt. X 100.

Where NPs wt. is the weight of the recovered particles [25].

7. Evaluation of *In Vitro S. platensis* release:

The release of *S. platensis* extracts from polymeric NPs was studied in PBS at both (pH ~ 7.4) and (pH ~ 5.2). The freeze-dried NPs were dispersed in 5 mL of 1X PBS. The temperature of the setup was adjusted to 37°C in the dark with mild shaking. 0.5 mL aliquots were collected at programmed time intervals and the release medium was refreshed with 0.5 mL of the medium after each withdrawal to maintain the total volume. Using the Nano-Drop®2000c Spectrophotometer (Thermo Fisher Scientific, USA) at wavelength 620 nm, together with the calibration curve of the encapsulation efficiency, another calibration curve at (pH ~ 5.2) was plotted and the unknown concentrations were calculated; hence the cumulative release of *S. platensis* extracts was determined.

8. RNA extraction and cDNA synthesis:

Total RNA was extracted from Caco-2, HepG-2, and Vero cell lines using Gene JET RNA Purification Kit (CAT#K0731, Thermo Fisher Scientific, USA) according to the manufacturer protocol. The concentration and purity of the extracted RNA were determined using Nano-Drop®2000c Spectrophotometer (Thermo Fisher Scientific, USA). Total RNA was reverse-transcribed to cDNA using the Revert Aid First Strand cDNA Synthesis Kit (CAT# K1622, Thermo Scientific, USA).

9. Quantitative Real-time PCR analysis:

Five µL of the cDNA were used for the real-time PCR amplification step using TNF-α, Caspase-3, and Cox-2 specific primers and master mix of (Maxima SYBR Green/ROX qPCR Master Mix 2X, Thermo Fisher, UK) using StepOne™ Real-Time PCR System (AB Applied Biosystems, Foster City, CA, USA). Beta-actin was used as a housekeeping gene and was utilized as a reference are all the used genes (Table 1). The real-time PCR program was carried out with an initial denaturation at 95°C for 10 min, annealing at 56°C for 30 seconds, and elongation at 72°C for 30 seconds through 50 cycles of PCR reaction. In the end, melting curve analysis was performed over a gradient holding out from annealing to a denaturation temperature. All reactions were run in duplicate. The ΔΔCT method was used for the relative quantification in all samples [26].

The list of PCR primer sequences

COX-2 forward primer

5´-CCC TTC CTT CGA AAT GCA AT-3´

Reverse primer

5´-CAT TTG AAT CAG GAA GCT GC-3´

TNFα forward primer

5´-ACA AGC CTG TAG CCC ATG TT-3´

Reverse primer

5´-AAA GTA GAC CTG CCC AGA CT -3

Caspase-3 forward primer:

5´-TGT TTG TGT GCT TCT GAG CC-3´

Reverse primer:

5´-CAC GCC ATG TCA TCA TCA AC-3´

B-actin forward primer

5´-TCT GGC ACC ACA CCT TCT ACA ATG-3´

Reverse primer

5´-AGC ACA GCC TGG ATA GCA ACG-3´

10. GC-MS Analysis of 90% MeOH ext. of *Spirulina platensis*:

Chromatographic analysis using GC–MS was performed (Agilent Technologies 7890B GC Systems combined with 5977A Mass Selective Detector). Capillary column was used (HP-5MS Capillary; 30.0 m × 0.25 mm ID × 0.25 µm film). Helium was used also as a carrier gas at a pressure of 8.2 psi with 1 µL injection. The sample was analyzed with the column held initially for 3 min at

60°C after injection, then the temperature was increased to 300°C with a 15°C /min heating ramp, with a 5.0 min hold. The injection was carried out in split-less mode at 300°C. MS scan range was (m/z): 50–550 atomic mass units (AMU) under electron impact (EI) ionization (70 eV) and solvent delay of 8.0 minutes.

Silylation agent: N, O-Bis (trimethylsilyl) trifluoroacetamide (BSTFA) with trimethylchlorosilane (Sigma -Aldrich)

The reaction was carried out by adding 300 µL of BSTFA to an amount of the extracted sample, the mixture was heated in a water bath at 80°C for two hrs, then injected into GC/MS under the above conditions. The constituents were determined by mass fragmentation with the NIST mass spectral search program for the NIST/EPA/NIH mass spectral library Version 2.2 (Jun 2014).

11. Statistical Analysis:

It was established by using Prism 8.0.2 program (ANOVA) for evaluating the means. All tests were performed in triplicate and presented as a mean ± standard deviation (SD). P-value < 0.01 represented a significant difference.

Results

1. *In-vitro* Assay for Cytotoxic Activity:

The cytotoxic effect of 90%MeOH ext. and its four derived fractions of *S. platensis* against HepG-2, Caco-2, and Vero cells was performed at different concentrations (6.25 µg/mL to 200 µg/mL). Results revealed that the MeOH ext. showed high cytotoxic activity against both cancer cells (75.5% against HepG-2 and 85.9% against Caco-2) at a concentration of 200 µg/mL. The half maximal inhibitory concentration (IC_{50}) values were calculated as the concentrations necessary to inhibit 50% of cell growth as compared to untreated control cells.

The IC_{50} of the 90%MeOH ext. in HepG-2 and Caco-2 was 65.2±3.5 and 39.3±0.6 µg/mL respectively. The cytotoxic activity of other fractions against HepG-2 cells was ordered as follows: pet-ether fr.> EtOAc fr.> BuOH fr. > water fr. However, the order was EtOAc fr. > BuOH fr. > pet-ether fr.> water fr. against Caco-2 cells while MeOH ext. and the other four fractions were safe on Vero cells (Table 1, Figure. 1).

2. Transmission electron microscope (TEM)

The results of the electron microscopy confirmed that the Nanometric size and the spherical morphology of the prepared empty CS-AlG NPs was (30.3±0.25 nm), MeOH ext. NPs were (35.4±0.9 nm) and the nanometric size of pet-ether fr. NPs were (31.17±0.6) as shown in Fig. 2a, 2b, and 2c. TEM analysis showed the capsular structure of the NPs due to the novel method, as it shows that the empty CS- ALG NPs, 90% MeOH ext. and pet-ether fr. NPs take a spherical shape with an inner dark portion of the drug encapsulated in a polymer shell, which is surrounded by the outer smooth layer of stabilizer that keeps the particles from aggregation and all NPs have an amorphous structure.

3. FTIR Analysis

The FTIR spectra of CS-ALG NPs, pet-ether fr., pet-ether fr. NPs, 90% MeOH ext. and 90%MeOH ext. NPs were as follows:

Empty Chitosan-Alginate NPs IR spectra revealed characteristic absorption bands at wavelengths of 3360 cm-1 (NH2 and -OH groups stretching), 1650 cm-1 (amide I), 1500 cm-1 (Amide II), and 1377 cm-1 (Amide III). The characteristic peaks that appeared at 3363 cm-1 represent the -OH group, the stretching vibrations at 1000 cm-1 indicate the presence of C-O stretch of cyclic alcohols, and the stretching vibrations at 1610 cm-1 and 1005 cm-1 correspond to asymmetric and symmetric -COO - stretching vibration of carboxylate groups, respectively. The sodium alginate's saccharide structure is thought to be responsible for the strong band at 1024 cm -1 (C - O - C stretching). While the vibration bands at 3367 cm-1 suggest -OH stretching in non-encapsulated 90%MeOH ext. and pet-ether fr. FTIR spectrum, 2932 cm-1 (aromatic C-H stretching), 2885 cm-1 (aliphatic C-H stretching), 1620 cm-1, and 1455 cm-1 (aromatic C=C stretching), respectively. CS and ALG complexation in the enclosed structure of 90%MeOH ext. and pet-ether fr., as well as the observation of loaded nanoparticles, may be the cause of the powerful band at 1025 cm-1 and 2880 cm-1. Intense peaks at 1660 cm-1 and 1720 cm-1 in the spectra of the final build show the chemical interaction of the extract and its derived fraction with polymers in the intricate polymeric network [27]. 90%MeOH ext. and pet-ether fr. were physically confined in the polyelectrolyte complex, as demonstrated by FTIR, without forming any chemical complexes with the polymers (Figure. 3).

4. Drug Release

In this study, the ratio of AlG: CS was adjusted at 1:2 to achieve a highly controlled *in vitro* release profile of *S. platensis*/CS-ALG NPs in PBS at pH 7.4 (normal cells) and pH 5.2 (cancer cells). The *in vitro* release profile was demonstrated for the two examined pH, a continuous and well-ordered release occurred for a period time of 144 hrs.

The *S. platensis* /CS-ALG NPs showed an initial release of 32.81, 37. 95% for 90%MeOH ext. NPs and 17.18, 17. 93% for pet-ether fr. NPs at pH

7.4 and pH 5.2, successively in 24 hrs. 49.9, 50. 65% for MeOH ext. NPs and 38.75, 40.14% for pet-ether fr. NPs within 72 hrs and a cumulative release of 95.25, 97.5% for 90% MeOH ext. NPs and 92.25, 94.25% for pet-ether fr. NPs by 7 days (Figure. 4).

The release study clarifies that the loaded *S. platensis* onto CS-ALG delivery system was more poorly released in normal cells (pH 7.4) than that in the cancer cell (pH 5.2), and the NPs loaded with 9%MeOH ext. showed very well sustained release, whereas those of the petroleum ether fraction showed delayed release.

5. Anti-cancer Activity of 90% MeOH ext. and pet-ether fr. NPs

The cytotoxic effect of 90%MeOH ext. NPs and pet-ether fr. NPs against HepG-2, Caco-2, and Vero cells were performed at different concentrations (6.25 µg/mL to 200 µg/mL). Results revealed that the MeOH ext. NPs showed a high cytotoxic effect against HepG-2 of about 87.0% and 94.3% against Caco-2, while that of pet-ether fr. NPs was 73.1% against HepG-2 and 87.5% against Caco-2 at concentration 200 µg/mL. The IC_{50} of the 90%MeOH ext. NPs in HepG-2 was 48.0±0.18 and in Caco-2 was 30±0.16 µg/mL, the IC_{50} of Pet-ether fr. NPs was 73.6±1.52 and in Caco-2 was 65.2±0.25 µg/mL. While all the tested compounds were safe on normal Vero cells with IC_{50} > 500 µg/mL (Table 2, Figure. 5)

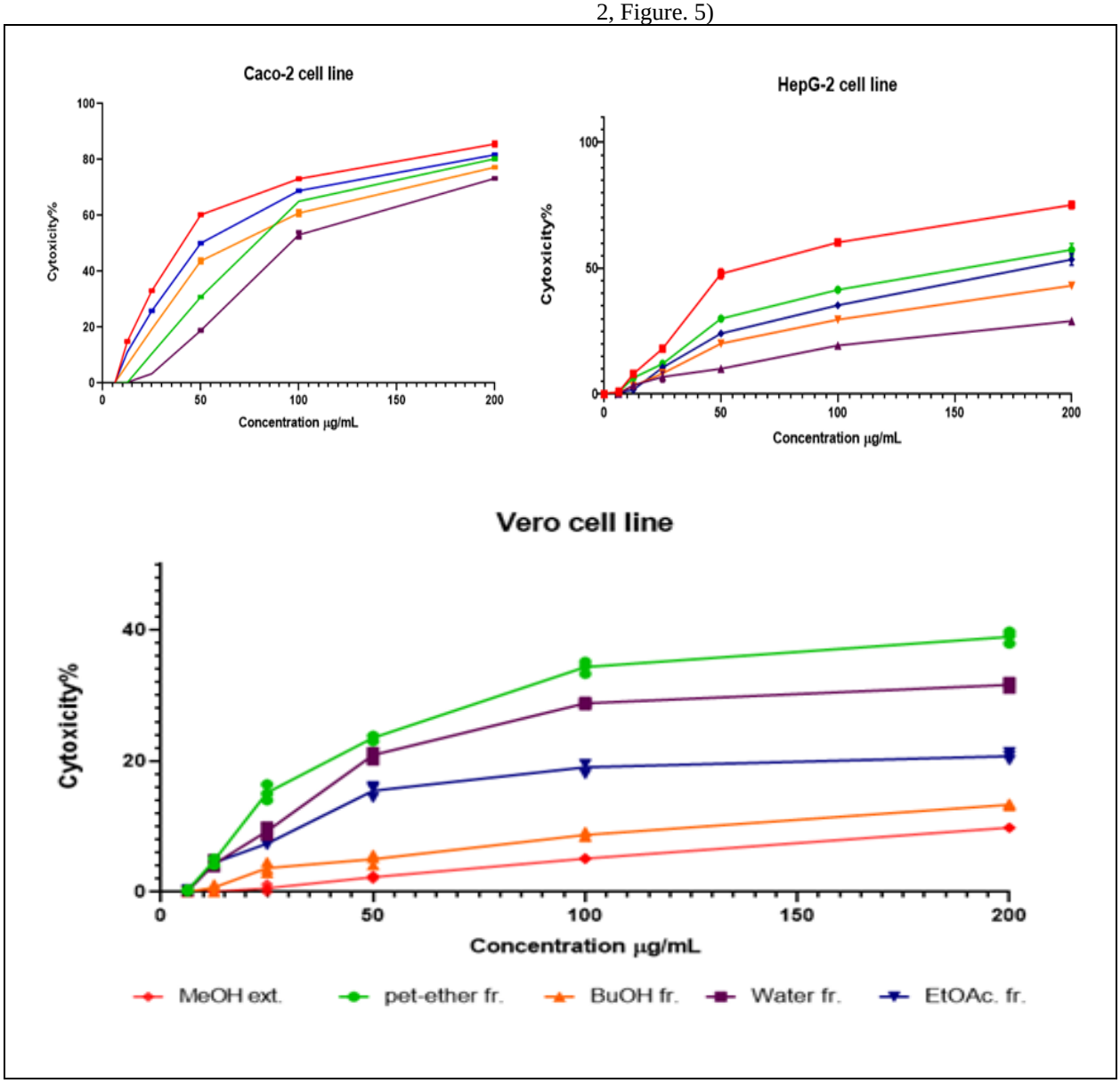

Figure 1: Evaluation of the cytotoxicity with different concentrations of 90%MeOH ext. of *S. Platensis* and its different derived four fractions on HepG-2, Caco-2, and Vero cells respectively after 72 hrs incubation.

Table (1): *In-vitro* cytotoxic activity of *S. platensis* extracts against HepG-2, Caco-2, and Vero cells.

Concentration (µg/mL)	200	100	50	25	12.5	IC_{50} (µg/mL)
HepG2						
90%MeOH ext.	75.5±1.47	60.2±0.46	47.8± 2.0	18.1±0.17	8.09±0.14	65.2±3.5
Water fr.	29.05±0.93	19.3±1.15	10.10±0.1	6.89±1.9	3.61±1.2	538.55±45.6
BuOH fr.	43.12±0.08	29.6±0.20	20.1±0.15	8.24±0.25	3.2±0.25	195.1±2.2
EtOAc fr.	53.5±2.21	35.3±0.66	24.1±0.17	10.6±0.01	1.74±0.05	177.7±1.8
Pet-ether fr.	57.4 ±2.45	41.4±0.57	30±0.07	12.1±0.17	6.5±0.1	140.7±1.0
Caco2						
90%MeOH ext.	85.9 ±0.50	73.1±0.14	60.2±0.187	33.04±0.064	14.9±0.09	39.3±0.6
Water fr.	73.2±0.051	53.07±1.01	18.85±0.14	3.35±0.002	0.306±0. 024	97.5±1.8
BuOH fr.	77.2±0.052	60.8±0.74	43.70±0.60	19.3±0.005	6.62±0. 05	68.6±1.10
EtOAc fr.	81.7±0.07	68.8±0.09	50.08±0.07	25.8±0.08	11.12±0.1	49.5±1.6
Pet-ether fr.	80.3±0.21	65.05±0. 96	30.8±0.05	10.56±0.20	0.20±0.8	73.6±0.3
Vero						
90%MeOH ext.	9.80±0.013	5.10±0.0	2.26±0.25	0.6±0.01	0.033±0.057	944.29±3.9
Water fr.	31.6±0.52	28.76±0.25	20.9±0.6	9.26±0.7	4.26±0.64	382.89±2.1
BuOH fr.	13.3±0.2	8.7±0.43	5.0±0.81	3.6±0.86	0.7±0.6	647.68±3.2
EtOAc fr.	20.7±0.6	19.0±0.8	15.4±0.9	7.4±0.2	4.46±0.25	644.65±3.4
Pet-ether fr.	38.9±0.91	34.3±0.9	23.4±0.4	15.13±1.2	4.8±0.6	237.82±1.6

Values are presented as mean ± SD, the test was performed in triplicate for each group, and all results were significantly different with a P-value <0.0001.

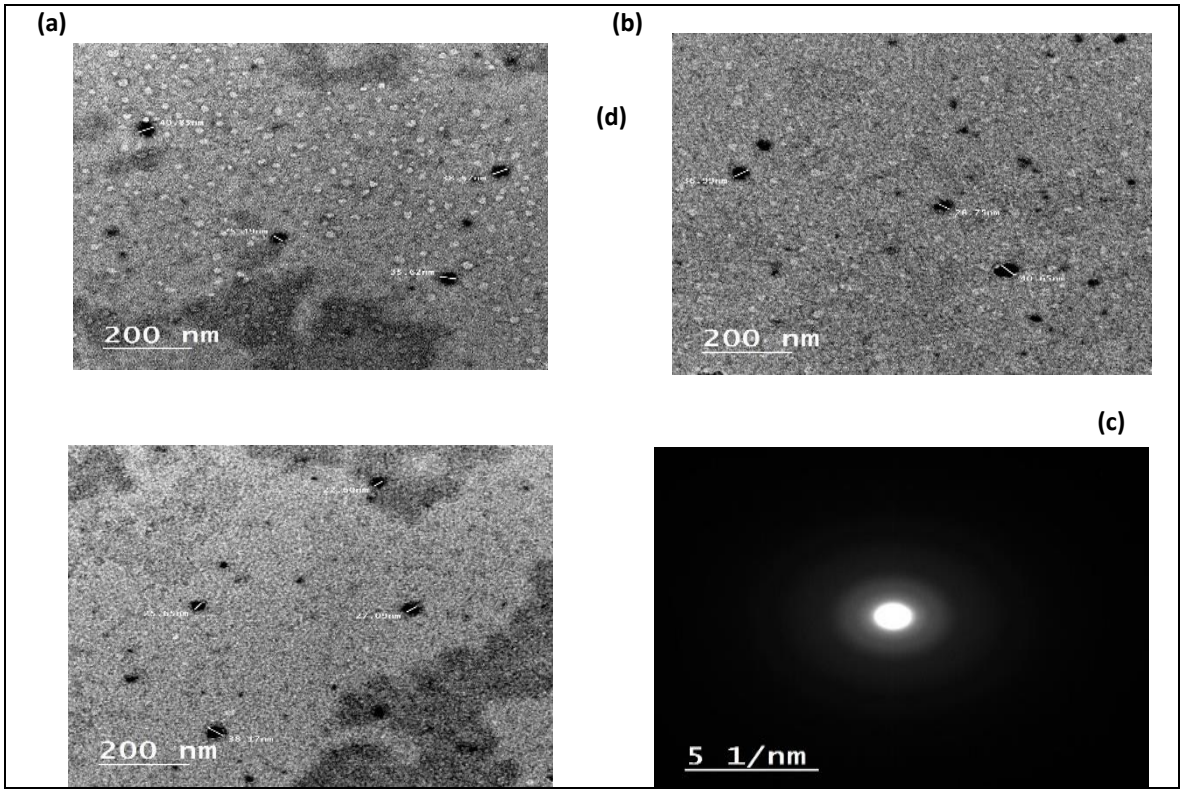

Figure 2: Transmitted Electron Microscope image of **(a) 90%**MeOH ext. NPs **(b)** pet-ether fr. NPs **(c)** empty CS /ALG NPs **(d)** the amorphous phase of NPs.

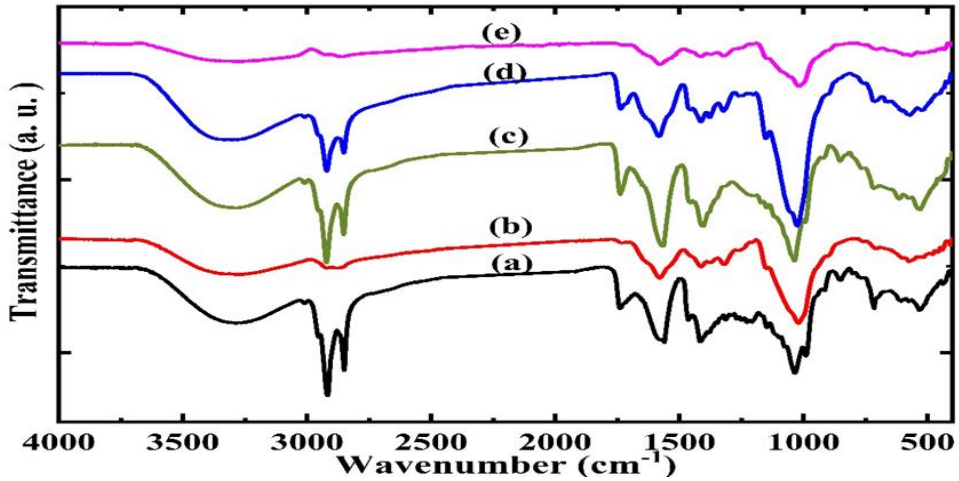

Figure 3: FTIR spectra of (a) pet-ether fr. (b) pet-ether fr. NPs (c) 90% MeOH ext. (d) 90% MeOH ext. NPs (e) empty CS-ALG NPs.

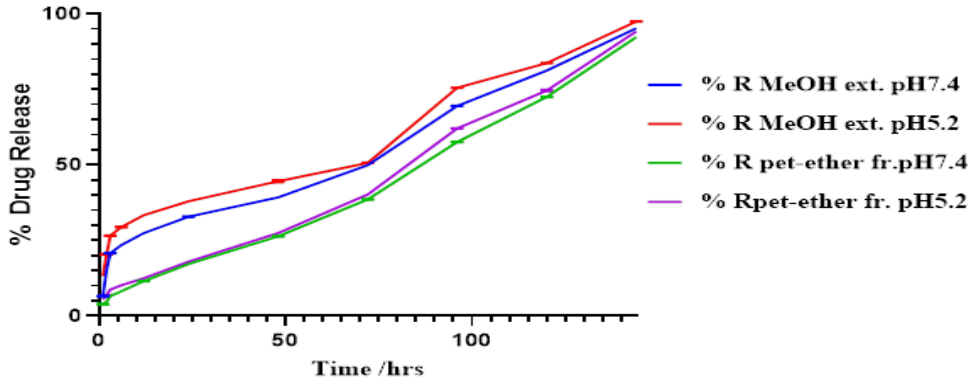

Figure 4: *In vitro* cumulative release profiles of 90%MeOH ext. and pet-ether fr. from loaded CS-ALG NPs at various pH media at 37°C ± 0.5°C (pH 5.2, 7.4).

Table (2): *In-vitro* cytotoxic effect of CS-ALG 90% MeOH ext. NPs and pet-ether fr. NPs against HepG-2, Caco-2, and Vero cells

Concentration (µg/mL)	200	100	50	25	12.5	IC50 (µg/mL
HepG2						
90%MeOH ext. NPs	87.01±0.016	68.01±0.023	54.02±0.028	34.12±0.123	20.123±0.118	48.0±1.8
pet-ether fr. NPs	73.120±0.91	58.25±0.9	43.05±0.4	15.15±1.2	7.05±0.6	73.6±1.5
Empty NPs	33.46±0.47	21.30±0.08	11.52±0.307	0.794±0.054	0.24±0.01	278.8±3.5
Caco2						
90%MeOH ext. NPS	94.3±0.13	81.0± 0.057	67.33± 0.30	48.1± 0.55	20.3± 0.56	30±0.16
pet-ether fr. NPs	87.5±0.26	76.2±0.11	35.5±0.38	14.67±0.20	0.54±0.006	65.2±0.25
Empty NPs	30.35±0.19	15.45± 0.21	6.36± 0.027	1.86± 0.5	1.34± 0.07	322.9±4.5
Vero						
90%MeOH ext. NPS	16.6±0.01	3.23±0.15	0.433±0.15	0.133±0.057	0.077±0.067	616±5.9
pet-ether fr. NPS	20.05±0.06	4.04±0.07	0.303±0.049	0.215±0.025	0.036±0.06	513±2.5
Empty NPs	16.1±0.09	2.4±0.1	0.23± 0.057	0.20±0.01	0 ± 0	630±3.6

Values are presented as mean ±SD, the test was performed in triplicate for each group, and results were significantly different with a P-value <0.0001.

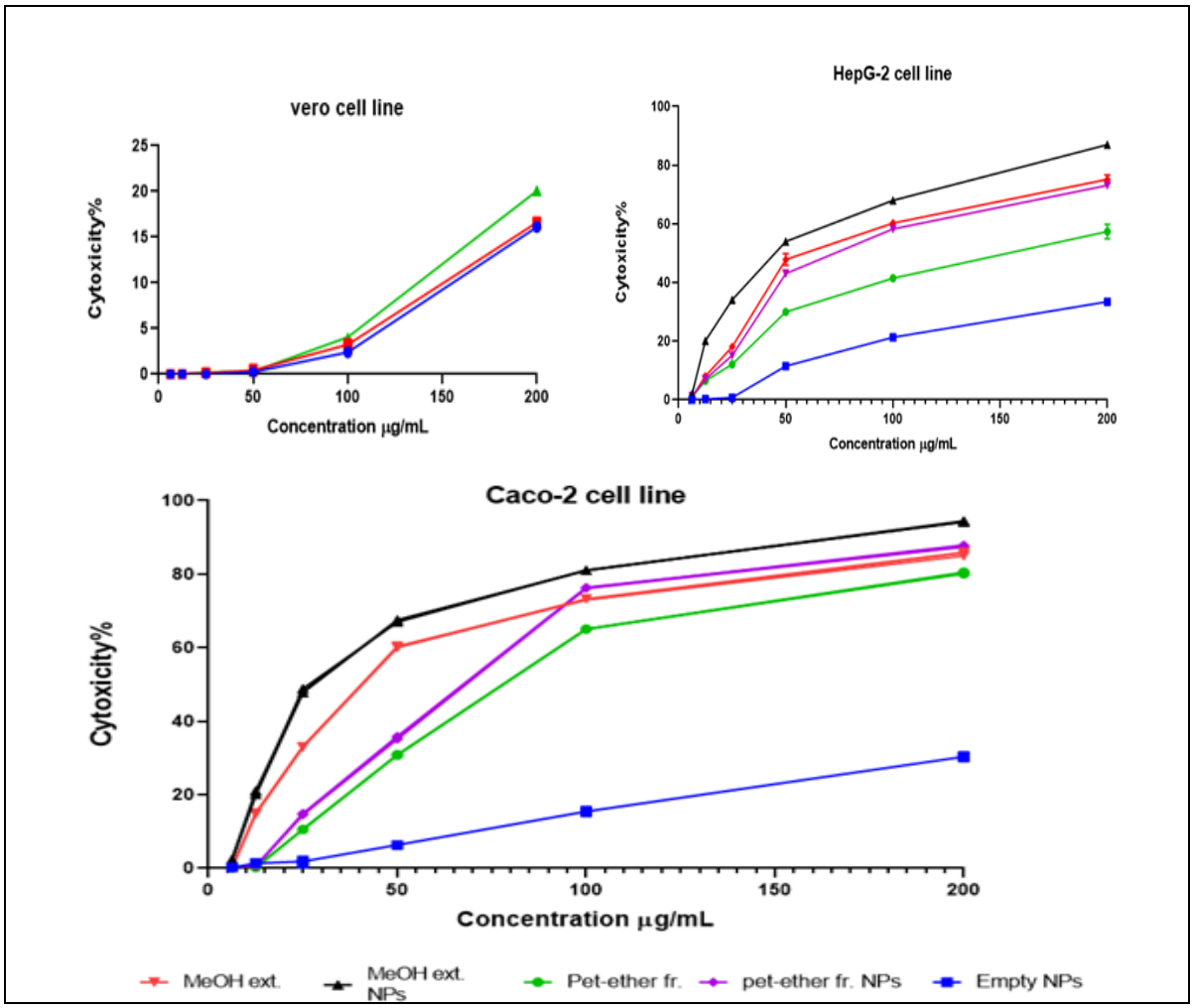

Figure 5: Cytotoxic effect of 90%MeOH ext. and pet-ether fr. encapsulated and non- encapsulated compared to empty CS-ALG NPs' on HepG-2, Caco-2 and Vero cells respectively.

1. Quantitative Real-time PCR analysis

Encapsulation of 90%MeOH ext. of *S. platensis* by CS-ALG NPs showed a downregulation expression of TNF-α in Caco-2 cells by 89.4%, while the non-encapsulated produced 73.7% downregulation. On the other hand, the encapsulated pet-ether fr. produced a decrease of 79.0%, while the downregulation expression percentage of the non-encapsulated fraction was 57. However, in HepG-2 cells, the encapsulated 90%MeOH ext. showed downregulation of TNF-α by 84.9% compared to 61.2% produced by the non-encapsulated extract. The encapsulated pet-ether fr. showed 56.2% while non-encapsulated produced 31.4% compared to the cell control (Figure 6a).

Regarding the expression of COX-2, after 72 hrs treatment of Caco-2 cells with encapsulated 90%MeOH ext. and pet-ether fr., results showed that the expression decreased by 86.2% and 71.1% respectively compared to the cell control, while treatment with non- encapsulated 90%MeOH ext. and pet-ether fr. caused a further downregulation in the COX-2 expression by 60.3% and 47.4% respectively. The same pattern was reflected on HepG-2 cells, where the COX-2 expression was downregulated by 90% MeOH ext. and pet-ether fr. and their encapsulation pattern in this descending order by 39.3%, 15.6% and 60.7%, 43.3%, compared to the control group as shown in (Figure 6b). The caspase-3 enzyme, which is an important parameter in the apoptotic pathway, showed higher expression in the encapsulated 90%MeOH ext. and the pet-ether fr. of *S. Platensis* than the non-encapsulated treatment in both cell lines normalized to the cell control, while in Caco-2 the expression of caspase-3 was higher than that in HepG-2 cells by six folds change as shown in (Figure 6c).

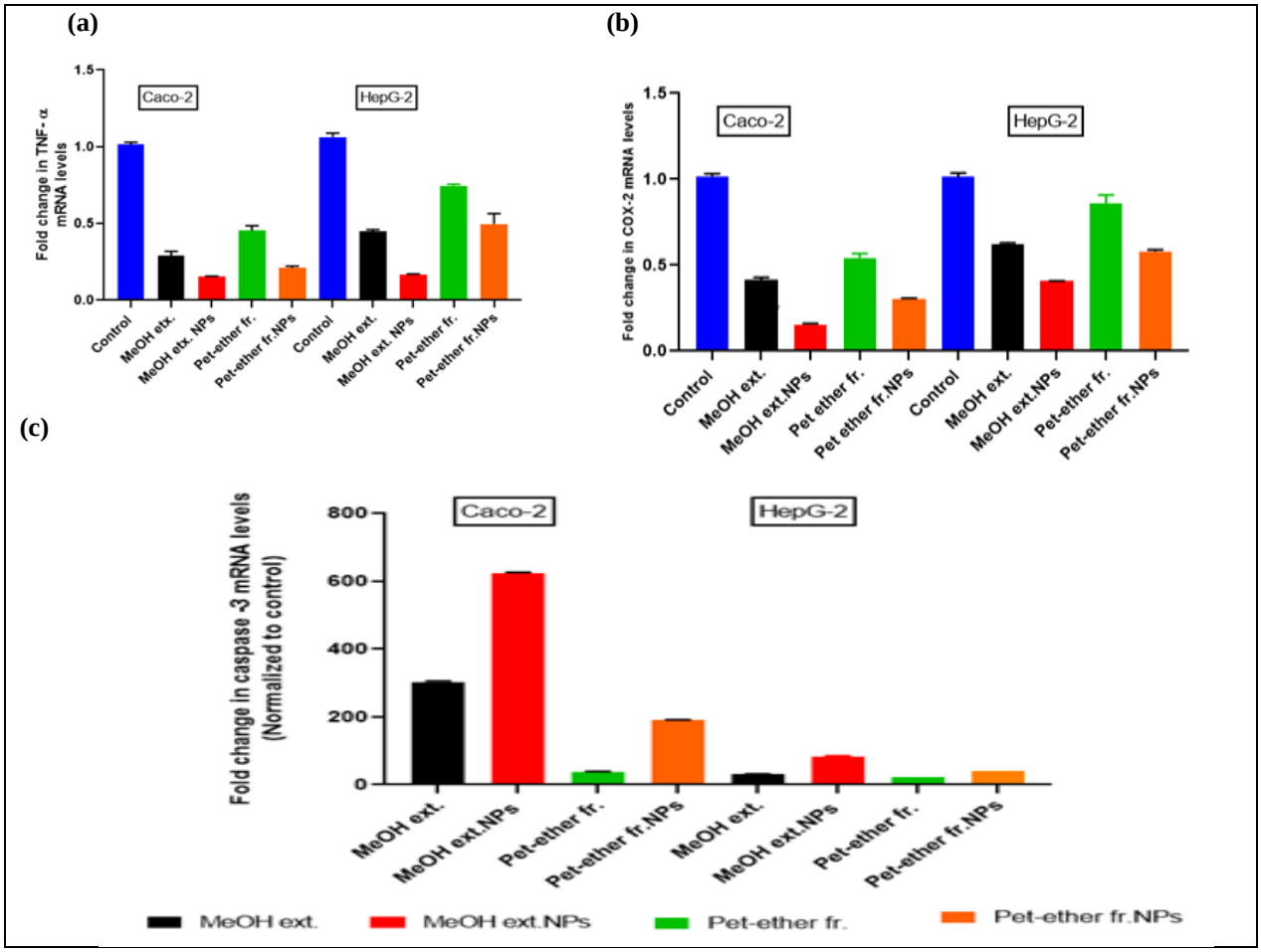

Figure 6: Gene expression level of (a) TNF-α (b) COX-2 and (d) Caspase-3 after treatment of Caco-2 and HepG-2 cells for 72 hrs with IC_{50} Concentrations of encapsulated and non-encapsulated 90% MeOH ext. and pet-ether fr. of *S. platensis* algae. All data were made in triplicate and expressed as mean ± SD and statistically significant with ($P<0.05$)

Table (3) mRNA expression levels of TNF-α, COX-2 and Caspase-3 apoptotic gene in *S. platensis* 90%MeOH ext. and Pet-ether fr. before and after encapsulation by CS-ALG NPs.

Genes	TNF-α	COX-2	Caspase -3
HepG2			
Cell control	1.06±0.02	1.01±0.015	1.02±0.03
90%MeOH ext.	0.448±0.013	0.62±0.01	31.4±0.2
90%MeOH ext. NPs	0.169±0.003	0.406±0.002	83.7±1.53
pet-ether fr.	0.74±0.010	0.86±0.05	21.81±0.02
pet-ether fr. NPs	0.498±0.07	0.58±0.01	40.4±0.1
Caco2			
Cell control	1.05±0.038	1.04±0.01	1.02±0.02
90%MeOH ext.	0.28±0.01	0.414±0.015	302.6±3.055
90%MeOH ext. NPs	0.15±0.01	0.155±0.006	624.6±1.528
pet-ether fr.	0.45±0.03	0.54±0.025	38.9±0.361
pet-ether fr. NPs	0.23±0.04	0.306±0.002	189.67±2.51

Values are presented as mean ±SD, the test was performed in triplicate for each group, and results were significantly different with p-value <0.001.

2. GC-MS analysis of 90% Methanolic extract of *S. platensis*

The GC-MS analysis of the silylated constituents of *S. platensis* 90 % MeOH ext. with its retention time (RT), concentration (area %), molecular formula (MF), and molecular weight (MW) are presented in table 4, figure 7. The results indicated the presence of 57 bioactive compounds identified as fatty acids, fatty acid esters, amides, alcohols, terpenes, amines, organic acids, and polysaccharide compounds which represent 96.63% of total volatile constituents. The most abundant compounds were α-D-Galactofuranose, 1, 2, 3, 5, 6-pentakis-O-(trimethylsilyl) which represent 9.50% followed by 9,12-octadecadienoic acid (Z, Z)-, methyl ester (8.54%), hexadecanoic acid, methyl ester (7.55%), pyrimidine-2-amine, 4-methyl-6-(2-pyridylthio)- (6.48%), palmitic Acid, TMS derivative (6.43%), 9,12-octadecadienoic acid (Z, Z)-, TMS derivative (5.76%), (+/-)-3-hydroxybutyric acid, 2TMS derivative (5.53%), D-(+)-talofuranose, pentakis(trimethylsilyl) ether (isomer 2) (5.15), Melibiose, octakis (trimethylsilyl)- (4.34%) and Glyceryl-glycoside TMS ether (4.09%).

Discussion

Microalgae and other cyanobacteria are significant sources of natural products with extraordinary biological properties. There are numerous antioxidants produced by various types of microalgae, each with a different concentration. [28].

S. platensis, a well-known cyanobacterium, is a multicellular filamentous, spiral-shaped, photosynthetic organism that can thrive in freshwater, marshes, and ocean water [29].it is a marine microalga with a long history of being safely ingested by humans.*S. platensis* can be used as an excellent source of protein, beta-carotene, vitamins, and minerals for functional food ingredients, animal feed, and medication. [30].

Also, *S. platensis* has several pharmacological activities, including antibacterial, antioxidant, anti-inflammatory, anti-aging, and anticancer qualities [31].

The major aim of this work was to extract and characterize the bioactive components of *S. platensis* algae and evaluate the biological and anticancer activities of this extract after encapsulation by CS-ALG NPs.

Kavisri et al.[32]used methanol to extract *S. platensis* to study its antibacterial and antioxidant properties as well as the structural makeup of the methanolic extracts, and the yield was estimated at 16%.

However, the extraction yield was 30.8%, which was consistent with the extraction technique. Moreover, in our study, the 90% MeOH ext. from *S. platensis* algae can inhibit the proliferation of HepG-2 and Caco-2 cells and showed greater anticancer activity than other derived fractions. While the cytotoxic activity of other fractions in the HepG-2 cell line was ordered as follows: pet-ether fr..> EtOAc fr.> BuOH fr. > water fraction. However, the order was EtOAc fr.> BuOH fr. > pet-ether fr.> water fr. in Caco-2 cell line. The results also indicated that *S. platensis* extract and its fractions inhibited only the growth of HepG-2 and Caco-2 but did not significantly affect the proliferation and morphology of Vero cells.

Our results were parallel with those of Challouf et al.[33] who reported that the biological and cytotoxic effect of extracellular polysaccharides of MeOH ext. of *S. platensis* against the Caco-2 cell line was 75.75%.

The current results are in agreement with those of [34] who determined the cytotoxic effect of *S. platensis* ext. against HepG-2 cells that showed inhibition of 68% with a concentration of 100 µg/mL. While our results disagree with [35] who reported that MeOH ext. of *S. platensis* has no cytotoxic effect against the colon cancer cell line.

Moreover, one of the challenges in creating an efficient drug delivery system is managing the release of the medication. To do this, a large number of multifunctional NPs have been developed, each with a different trigger and set of associated chemistries. To administer medicine with the most potent and long-lasting therapeutic effect, a trigger-dependent drug delivery system is preferred [36].

Recently, polymer-based NPs have attracted a lot of attention as a potential medication delivery mechanism. Because polymers are distinctive nanoparticles with a distinctive nanostructure consisting of a polymeric shell encircling a liquid or solid core, drug delivery techniques in polymers are becoming more and more fascinating [37].

Alginate and chitosan are examples of materials that are appropriate for making NPs because they have many benefits such as fast gelation, enhanced biocompatibility, and reduced toxicity. Nonetheless, they are used in hydrogel for objectives including regulating medicine release and tissue engineering [38].

In this study, to increase the hydrophilic drug's therapeutic effect against cancer cell lines, a novel technique was used, this technique was based on encapsulation of the hydrophilic 90% MeOH ext. of *S. platensis* and its pet-ether fr. with a high drug encapsulation efficiency to make it available at a slower drug release level.

The treatment's effectiveness and cellular absorption can be significantly impacted by the size, shape, and surface chemistry of NPs [39]. In the present study, the average diameter of the prepared 90% MeOH ext. NPs and pet-ether fr. NPs were 35.4 nm and 31.17 nm respectively. While that of empty CS-ALG polyelectrolyte NPs was 30.3 nm, the bigger size of *S. platensis* NPs compared to empty ones indicates the incorporation of the drug inside the NPs.

The current results revealed that the obtained *S. platensis* /CS-ALG NPs had a suitable size for use in therapeutic applications and could be useful for the treatment of liver and colon cancers.

The obtained results were more efficient than Katuwavila et al. [23] 's results, which developed polymeric NPs of CS-ALG with a mean particle size (100±28)nm.

Our results are inconsistent with [40] who reported that the polymeric NPs prepared using the ionotropic gelation method typically have mean particle sizes between 480.9 and 695 nm. The present study showed that the encapsulation efficiency of 90% MeOH ext. NPs was 96% and 95% for pet-ether fr. NPs and the drug loading was 23% for MeOH ext. NPs and 24% for pet-ether fr. NPs, the increase in the encapsulation efficiency may be due to the use of a novel method. While the efficiency of the novel bio-polymeric complex multi-particulate system consisting of CS-ALG NPs used in the treatment of colon cancer was 85.63% according to [41].

As was published by Jyothi et al. [42], the variables that have an impact on how well a microparticle, microsphere, or microcapsule encapsulates an object is the concentration of the polymer, the solubility of the polymer in the solvent, the rate of solvent removal and the solubility of organic solvent in water as the presence of tween 80 in chitosan solution which plays a good role to make the particle size very small. The release of drugs from the CS-ALG NPs is affected by the hydrophilicity of chitosan and the pH of the swelling solution.

Therefore, a modified drug release can be achieved when polymers get into contact with an aqueous medium, the polymer swells get degraded and followed by the diffusion of drugs through the cell matrix in the site of disease[43].

Due to the hydrophilicity of chitosan, CS-ALG NPs exhibit pH-dependent drug and controlled drug release systems [44].

In a previous study by Yin et al.[45], who reported that CS-ALG composite particles with a high weight ratio of ALG to CS had a lower release rate. This may be mostly due to the insolubility of chitosan-coated on NPs in neutral solvents, which prevents ALG from absorbing solvents, swelling, and releasing the CS until the degradation of chitosan. After the degradation of the outer chitosan, the release resistance of CS is mainly related to the swelling of cross-linked ALG. The higher the ratio of ALG: CS, the greater the resistance of CS release and the slower the release rate.

The exponential pattern demonstrated by the release profile of *S. platensis* /CS-ALG NPs indicates that the system is suitable for the sustained release of therapeutics. The amount of *S. platensis* and chitosan as well as the degree of deacetylation of chitosan plays a vital role in the release rate. The higher deacetylation of chitosan, the higher the number of amino groups that form ionic interactions with negative carboxyl groups of sodium alginate, resulting in the formation of dense particles which leads to lower permeability of NPs surface and a decrease in release rate. Our findings were supported by Kafshgari et al.[46] who concluded that the larger amount of encapsulated *S. platensis* leads to a higher diffusion rate due to the formation of a concentration gradient between the chitosan and buffer matrix. Since the MeOH ext. NPs and pet-ether fr. NPs were high amounts and showed 95% and 96% entrapment efficiency respectively, and the release rate was slow, this is because the chitosan used in this study is of low concentration (2 mg/mL) and a high degree of deacetylation.

In our study, the cytotoxic effect of 90%MeOH ext. NPs and pet-ether fr. NPs against HepG-2, Caco-2, and Vero cells at different concentrations showed that they have high cytotoxic activity than non-encapsulated fractions. While all the tested compounds did not affect the viability of normal Vero cells with IC50 > 500 µg/mL.

Furthermore, our results are inconsistent with the findings of İnan et al. [47] as they tested the particles only against HepG2 cells and indicated inhibition rates of non-encapsulated, microencapsulated, and nano-encapsulated products on HepG2 cells were found as 47.9, 38, and 31%, respectively.

In our study, treatment of HepG-2 and Caco-2 with *S. platensis* and its derived fractions has shown a significant decrease in the surviving fraction of both cells and increased cell death that could be explained by a decrease in the concentration of gene expression of TNF-α and a decrease in the target gene transcription including cyclooxygenase -2 enzyme (COX-2) inhibitors play a good role in reducing the risk of colon, liver cancer and act as effective chemopreventive moreover, there was a significant increase and up-regulation in the gene expression of caspase-3 enzyme that is a well-known important enzyme involved in the intrinsic pathway of apoptosis (programmed cell death).

As our investigation is compatible with the result of Herrero et al. [5] that showed that the decreased level of cytokines that stimulate TNF-α, lowered protein levels of activated transcription factors (STAT3 AND NF-kB) and decreased protein expression level of COX-2 and TNF-α genes confirm the inhibition of the key pathways in tumor progression and promotion in colon and liver.

Furthermore, the effect of encapsulation of the 90%MeOH ext. of *S. platensis* algae with CS /ALG polyelectrolyte NPs and its derived pet-ether fr. showed more downregulation and decreased in the relative expression of TNF-α and COX-2 and higher upregulation in the expression of caspase-3 enzyme. *Spirulina platensis* is an abundant source of nutritional composition, including proteins, vitamins, lipids, filaments, minerals, carbohydrates, and some natural colors. These main ingredients confer a physiological eventuality and a functional benefit that make it

promising for food assiduity to overcome the problem of malnutrition and in health operations against numerous conditions [13]. In the present study, the 90% MeOH ext. of *S. platensis* was subordinated to the silylation process, which has been extensively used especially in the determination of low- volatility polar composites which show low discovery perceptivity. The silylation procedure makes it simple to produce thermally stable and largely unpredictable composites. numerous silylation reagents are used for the derivatization of the hydroxyl group including bis(trimethylsilyl) trifluoroacetamide(BSTFA), which have been extensively used because of their fast responses with colorful hydroxyl composites at moderate conditions[48]. thus, the GC- MS analysis of *90*% MeOH ext. revealed so numerous silylated composites as shown in table 5. The relative probabilities of the composites are given in Table(5). The most current composites were α- D-Galactofuranose,- pentakis- O-(trimethylsilyl),,12-Octadecadienoic acid(Z, Z)-, methyl ester, and Hexadecanoic acid, methyl ester. The preliminarily reported study carried out by Agustini et al. [49] showed the identification of thirteen bioactive composites from the incompletely purified fragments of the cyanobacterium S.platensis. The most current emulsion was n- Hexadecanoic acid(34.28). While, Deyab et al. [50] reported that the major chemical ingredients of *S. platensis* 90% MeOH ext. were 12-Octadecadienoic acid(Z, Z)-, methyl ester(30.3%) followed by Hexadecanoic acid, methyl ester(29.26%), 9- Octadecenoic acid, methyl ester(20.22%). Also, Cai et al [51] reported that *S. platensis* is rich in proteins(60 – 70%), polysaccharides(15 – 20%), and other nutrients, which are generally consumed as a nutraceutical food supplement.

Conclusion

Cyanobacteria family has been widely used in conventional medicine, *S. platensis* one member of this family, our present study on the 90%MeOH ext. and its fractionated extracts reveals the importance of *S. platensis* algae in manufacturing new pharmaceuticals, especially anticancer drugs, and demonstrates its vital phytochemicals. *S. platensis* was estimated for its therapeutic activity, 90%MeOH ext. and pet-ether fr. were the most active extracts as anti-cancer. Encapsulation of *S. platensis* by CS-ALG NPs enhances and increases the anti-cancer effect, and the results assumed the potential therapeutic activity and put the basis for further studies on its bioactive compounds and its application in pharmaceutical purposes

4. Conflicts of interest:

The authors declare there are no conflicts of interest regarding the publication of this manuscript.

5. Formatting of funding sources

This work was funded by the Academy of Scientific Research and Technology (ASRT) through the program of Scientists for Next generation (SNG) master scholarship ID: FRM-SGO-22.

6. Acknowledgments

The corresponding author thanks a lot for the financial support of the Academy of Scientific Research and Technology (ASRT), professor Mohamed Hassoub and the team of the biochemistry and molecular biology department, Theodor Bilharz Research Institute especially Dr. Fatma Hassan, Specialist. Abdullah Elsayed Gouda for their help and support during the work.

Table (4). GC-MS analysis of different compounds of *S. platensis* 90% MeOH ext.

PK	RT		MW	MF	Peak Area %
1	7.66	(+/-)-3-Hydroxybutyric acid, 2TMS derivative	248	$C_{10}H_{24}O_3Si_2$	5.53
2	8.10	Pentasiloxane, dodecamethyl-	384	$C_{12}H_{36}O_4Si_5$	0.07
3	8.21	Arachidonic acid, TMS derivative	376	$C_{23}H_{40}O_2Si$	0.13
4	8.37	Butanedioic acid, 2TMS derivative	262	$C_{10}H_{22}O_4Si_2$	1.27
5	8.57	2-Pentamethyldisilanyloxybutane	204	$C_9H_{24}OSi_2$	0.02
6	8.70	Glycerol, 3TMS derivative	308	$C_{12}H_{32}O_3Si_3$	1.45
7	9.09	Butanedioic acid, 2TMS derivative isomer	262	$C_{10}H_{22}O_4Si_2$	1.06
8	9.24	Glyceric acid, 3TMS derivative	322	$C_{12}H_{30}O_4Si_3$	1.05
9	9.95	4-Dimethyl(trimethylsilyl)silyloxytridecane	330	$C_{18}H_{42}OSi_2$	0.08
10	10.10	(R*, S*)-3,4-dihydroxybutanoic acid triTMS	336	$C_{13}H_{32}O_4Si_3$	0.27
11	10.44	1-Ethyl-2-pentamethyldisilanyloxycyclohexane	258	$C_{13}H_{30}OSi_2$	0.12
12	10.58	3-Butenoic acid, 3-(trimethylsiloxy)-, trimethylsilyl ester	246	$C_{10}H_{22}O_3Si_2$	0.05
13	10.68	meso-Erythritol, 4TMS derivative	410	$C_{16}H_{42}O_4Si_4$	0.07
14	10.80	1-Octadecanol, TBDMS derivative	384	$C_{24}H_{52}OSi$	0.17
15	11.04	L-Threonic acid, tris(trimethylsilyl) ether, trimethylsilyl ester	424	$C_{16}H_{40}O_5Si_4$	0.85

16	11.27	Pentanedioic acid, 2-[(trimethylsilyl)oxy]-, bis(trimethylsilyl) ester	364	$C_{14}H_{32}O_5Si_3$	0.16
17	11.42	3-Hydroxybutyric acid, 2TMS derivative	248	$C_{10}H_{24}O_3Si_2$	0.52
18	11.81	4-Hydroxybenzeneacetic acid, 2TMS derivative	296	$C_{14}H_{24}O_3Si_2$	0.73
19	12.11	Heptadecane	240	$C_{17}H_{36}$	0.12
20	12.31	D-Xylopyranose, 4TMS derivative	438	$C_{17}H_{42}O_5Si_4$	0.26
21	12.77	Phosphoric acid, bis(trimethylsilyl) 2,3-bis[(trimethylsilyl)oxy] propyl ester	460	$C_{15}H_{41}O_6Psi_4$	1.42
22	13.10	Neophytadiene	278	$C_{20}H_{38}$	0.42
23	13.27	9-Tetradecenoic acid, (E)-, TMS derivative	354	$C_{14}H_{26}O_2Si$	0.20
24	13.41	9-Octadecyne	250	$C_{18}H_{34}$	0.23
25	13.59	α.-D-Xylopyranose, 4TMS derivative	438	$C_{17}H_{42}O_5Si_4$	0.52
26	13.75	Hexadecanoic acid, methyl ester	270	$C_{17}H_{34}O_2$	7.55
27	14.48	Palmitic Acid, TMS derivative	328	$C_{19}H_{40}O_2Si$	6.43
28	14.86	9,12-Octadecadienoic acid (Z, Z)-, methyl ester	294	$C_{19}H_{34}O_2$	8.54
29	15.49	9,12-Octadecadienoic acid (Z, Z)-, TMS derivative	352	$C_{21}H_{40}O_2Si$	5.76
30	15.68	Methyl galactoside (1S,2R,3S,4R,5R)-, 4TMS derivative	482	$C_{19}H_{46}O_6Si_4$	3.15
31	15.83	Glyceryl-glycoside TMS ether	687	$C_{27}H_{66}O_8Si_6$	4.09
32	16.25	Molybdenum, tricarbonyl [(1, 2,3,4,5, 6-.eta.)-1,4-dimethylbenzene]-	286	$C_{11}H_{10}MoO_3$	2.48
33	16.45	A-D-Glucopyranose, 2,3,4,6-tetrakis-*O*-(trimethylsilyl)-, bis(trimethylsilyl) phosphate	693	$C_{24}H_{61}O_9PSi_6$	2.00
34	16.74	Myo-Inositol, 1,3,4,5,6-pentakis-O-(trimethylsilyl)-, bis(trimethylsilyl) phosphate	765	$C_{27}H_{69}O_9PSi_7$	0.97
35	17.09	D-(-)-Tagatofuranose, pentakis(trimethylsilyl) ether (isomer 1)	540	$C_{21}H_{52}O_6Si_5$	0.55
36	17.28	Tetrachloro-*O*-benzoquinone	244	$C_6Cl_4O_2$	0.42
37	17.48	Pyrimidin-2-amine, 4-methyl-6-(2-pyridylthio)	218	$C_{10}H_{10}N_4S$	6.48
38	17.69	Ethyl 2-[4-chlorophenyl]-7,8-benzocinchoninate	361	$C_{22}H_{16}ClNO_2$	3.48
39	17.91	D-(-)-Lyxofuranose, tetrakis(trimethylsilyl) ether	438	$C_{17}H_{42}O_5Si_4$	4.75
40	18.24	α-D-Galactofuranose, 1,2,3,5,6-pentakis-*O*-(trimethylsilyl)	541	$C_{21}H_{52}O_6Si_5$	9.50
41	18.96	D-(+)-Talofuranose, pentakis(trimethylsilyl) ether (isomer 2)	541	$C_{21}H_{52}O_6Si_5$	5.15
42	19.31	2-α-Mannobiose, octakis(trimethylsilyl) ether (isomer 1)	918	$C_{36}H_{86}O_{11}Si_8$	0.53
43	19.48	D-(+)-Cellobiose, (isomer 2), 8TMS derivative	918	$C_{36}H_{86}O_{11}Si_8$	0.48
44	19.63	D-Glucose, 6-*O*- α -D-galactopyranosyl-, bis-*O*-(trimethylsilyl) deriv., cyclic tris(methylboronate)	558	$C_{21}H_{41}B_3O_{11}Si_2$	0.22
45	19.75	5,8,11-Eicosatrienoic acid, (Z)-, TMS derivative	378	$C_{23}H_{42}O_2Si$	0.58
46	20.07	2-*O*-Glycerol- α- d-galactopyranoside, hexa-TMS	686	$C_{27}H_{66}O_8Si_6$	1.41
47	20.44	Lactulose, octakis(trimethylsilyl) ether, methyloxime (isomer 1)	948	$C_{37}H_{89}NO_{11}Si_8$	0.33
48	20.79	D-Arabinopyranose, 4TMS derivative (isomer 2)	438	$C_{17}H_{42}O_5Si_4$	0.05
49	20.89	Altronic acid, gamma. -lactone, 4TMS derivavative	466	$C_{18}H_{42}O_6Si_4$	0.13
50	21.31	1,5-Anhydrohexitol, 4TMS derivative	452	$C_{18}H_{44}O_5Si_4$	0.09
51	21.49	Maltose, octakis(trimethylsilyl) ether, methyloxime (isomer 2)	947	$C_{37}H_{89}NO_{11}Si_8$	0.05
52	21.76	Moperone	355	$C_{22}H_{26}FNO_2$	0.05
53	21.90	3-α-Mannobiose, octakis(trimethylsilyl) ether (isomer 1)	918	$C_{36}H_{86}O_{11}Si_8$	0.12
54	22.12	Succinic acid, ethyl tetradec-11-enyl ester	340	$C_{20}H_{36}O_4$	0.03
55	22.47	β-D-Lactose, (isomer 2), 8TMS derivative	918	$C_{36}H_{86}O_{11}Si_8$	0.08
56	23.24	Melibiose, octakis(trimethylsilyl)-	918	$C_{36}H_{86}O_{11}Si_8$	4.34
57	23.60	Maltose, 8TMS derivative, isomer 2	918	$C_{36}H_{86}O_{11}Si_8$	0.12
Total					**96.68**

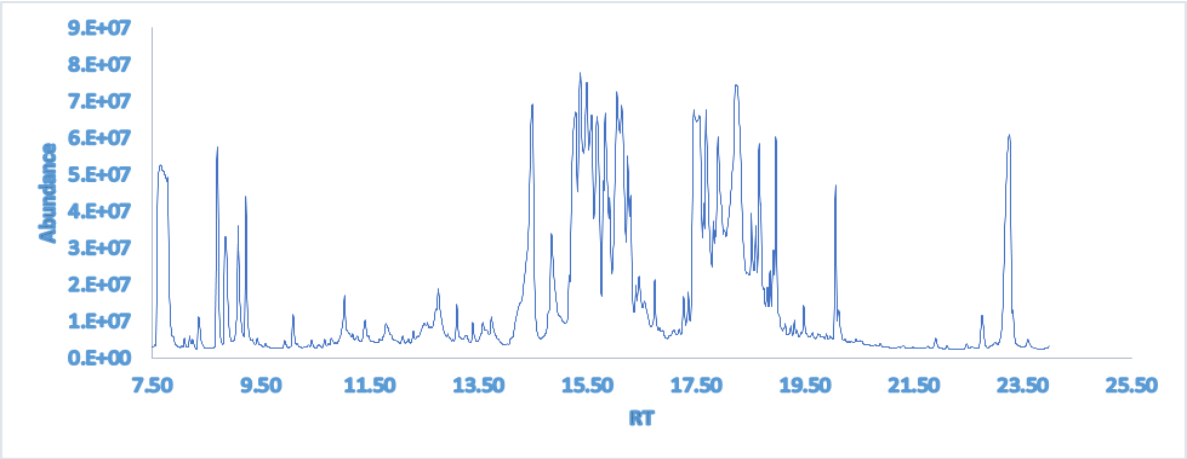

Figure7: GC-MS total ion chromatogram of *S. platensis* 90% MeOH ext.

References

[1] W. Zhu, Q. Zhang, M. Liu, M. Yan, X. Chu, and Y. Li, "Identification of DNA repair-related genes predicting vvvvvv cbzxcgpathogenesis and prognosis for liver cancer," Cancer Cell Int., vol. 21, no. 1, 2021.

[2] M. Hassan et al., "Drug response prediction of liver cancer cell line using deep learning," Comput. Mater. Contin. vol. 70, no. 2, 2022.

[3] M. E. Abd El-Hack et al., "Microalgae in modern cancer therapy: Current knowledge," Biomed. Pharmacother. vol. 111, no. October 2018, pp. 42–50, 2019.

[4] C. Y. Karakaş, H. Tekarslan Şahin, B. İnan, D. Özçimen, and Y. Erginer, "In vitro cytotoxic activity of microalgal extracts loaded nano–micro particles produced via electrospraying and microemulsion methods," Biotechnol. Prog, vol. 35, no. 6, pp. 1–8, 2019.

[5] A. Herrero, A. Benedicto, I. Romayor, E. Olaso, and B. Arteta, "Inhibition of cox-2 impairs colon cancer liver metastasis through reduced stromal cell reaction," Biomol. Ther. vol. 29, no. 3, 2021.

[6] J. Saha et al., "Propranolol Sensitizes Vascular Sarcoma Cells to Doxorubicin by Altering Lysosomal Drug Sequestration and Drug Efflux," Front. Oncol. vol. 10, 2021.

[7] A. F. U. H. Saeed, J. Su, and S. Ouyang, "Marine-derived drugs: Recent advances in cancer therapy and immune signaling," Biomed. Pharmacother. vol. 134, no. November 2020, p. 111091, 2021.

[8] A. Yücetepe, M. Yavuz-Düzgün, E. Şensu, F. Bildik, E. Demircan, and B. Özçelik, "The impact of pH and biopolymer ratio on the complex coacervation of Spirulina platensis protein concentrate with chitosan," J. Food Sci. Technol., vol. 58, no. 4, 2021.

[9] P. V. Yamgar and V. M. Dhamak, "Therapeutics role of spirulina platensis in disease prevention and treatment," IP Int. J. Compr. Adv. Pharmacol., vol. 7, no. 1, 2022.

[10] Y. L. Wang, G. S. Xi, Y. C. Zheng, and F. S. Miao, "Microwave-assisted extraction of flavonoids from Chinese herb Radix puerariae (Ge Gen)," J. Med. Plants Res., vol. 4, no. 4, pp. 304–308, 2010.

[11] A. Kumar et al., "Antioxidant and phytonutrient activities of Spirulina platensis," Energy Nexus, vol. 6, no. April, p. 100070, 2022.

[12] Y. Lu et al., "Spirulina polysaccharide induces the metabolic shifts and gut microbiota change of lung cancer in mice," Curr. Res. Food Sci., vol. 5, no. August, pp. 1313–1319, 2022.

[13] R. Seghiri, M. Kharbach, and A. Essamri, "Functional composition, nutritional properties, and biological activities of moroccan spirulina microalga," J. Food Qual., vol. 2019, 2019.

[14] T. Mutanda, D. Naidoo, J. K. Bwapwa, and A. Anandraj, "Biotechnological Applications of Microalgal Oleaginous Compounds: Current Trends on Microalgal Bioprocessing of Products," Front. Energy Res., vol. 8, no. December, pp. 1–21, 2020.

[15] G. Grasso, D. Zane, and R. Dragone, "Microbial nanotechnology: Challenges and prospects for green biocatalytic synthesis of nanoscale materials for sensoristic and biomedical applications," Nanomaterials, vol. 10, no. 1, 2020.

[16] H. Le, C. Karakasyan, T. Jouenne, D. Le Cerf, and E. Dé, "Application of polymeric nanocarriers for enhancing the bioavailability of antibiotics at the target site and overcoming antimicrobial resistance," Appl. Sci., vol. 11, no. 22, 2021.

[17] R. M. Alharbi, A. A. Soliman, and A. A. A. El Aty, "COMPARATIVE STUDY ON BIOSYNTHESIS OF VALUABLE ANTIMICROBIAL AND ANTITUMOR NANO-SILVER USING FRESH WATER GREEN AND BLUE-GREEN MICROALGAE," J. Microbiol. Biotechnol. Food Sci., vol. 10, no. 2, 2020.

[18] M. Jönsson, L. Allahgholi, R. R. R. Sardari, G. O. Hreggviosson, and E. N. Karlsson, "Extraction and modification of macroalgal polysaccharides for current and next-generation applications," Molecules, vol. 25, no. 4, 2020.

[19] U. States et al., "Современные Технологии in Vitro Тестирования Лекарств in Vitro: Использование Микробиореакторов," Биотехнология, vol. 12, no. 1, pp. 51–58, 2020.

[20] A. A. Omar, S. H. Ahmed, Y. E. A. Mobdy, H. A. Amra, and E. A. Abdel-Rahim, "Well-developed nanostructure incorporated with Euphorbia umbellata extract into a unique form with greater biocompatibility," Plant Cell Biotechnol. Mol. Biol., vol. 22, no. 27–28, 2021.

[21] F. H. Salman, E. A. Hassan, M. A. Mohamed, S. A. Sherif, M. N. Moharib, and E. M. A. El Azeem, "Evaluation of the Potential Therapeutic Anti-inflammatory, Anti- proliferative and Apoptotic Effects of Viburnum tinus Leaves Different Extracts.," Egypt. J. Chem., vol. 65, no. 4, 2022.

[22] Y. Zhou et al., "Studies on cytotoxic activity against HepG-2 cells of naphthoquinones from green walnut husks of Juglans mandshurica maxim," Molecules, vol. 20, no. 9, 2015.

[23] N. P. Katuwavila et al., "Chitosan-Alginate Nanoparticle System Efficiently Delivers Doxorubicin to MCF-7 Cells," J. Nanomater., vol. 2016, 2016.

[24] M. Akhtar, B. S. Murray, E. I. Afeisume, and S. H. Khew, "Encapsulation of flavonoid in multiple emulsion using spinning disc reactor technology," Food Hydrocoll., vol. 34, 2014.

[25] P. Koteš, J. Vičan, J. Prokop, and M. Strieška, "Determining load-carrying capacity and remaining lifetime of bridge in Vitanova, Slovakia," IOP Conf. Ser. Mater. Sci. Eng., vol. 365, no. 5, 2018.

[26] S. H. Kfir and I. Barash, "Calorie restriction and rapamycin administration induce stem cell self-renewal and consequent development and production in the mammary gland," Exp. Cell Res., vol. 382, no. 2, 2019.

[27] R. Sohail and S. R. Abbas, "Evaluation of amygdalin-loaded alginate-chitosan nanoparticles as biocompatible drug delivery carriers for anticancerous efficacy," Int. J. Biol. Macromol., vol. 153, pp. 36–45, 2020.

[28] J. F. López-Hernández, P. García-Alamilla, D. Palma-Ramírez, C. A. Álvarez-González, J. C. Paredes-Rojas, and F. J. Márquez-Rocha, Continuous microalgal cultivation for antioxidants production," Molecules, vol. 25, no. 18, 2020.

[29] M. Akbarizare, H. Ofoghi, M. Hadizadeh, and N. Moazami, "In vitro assessment of the cytotoxic effects of secondary metabolites from Spirulina platensis on hepatocellular carcinoma," Egypt. Liver J., vol. 10, no. 1, 2020.

[30] C. Ye et al., "Life cycle assessment of industrial scale production of spirulina tablets," Algal Res., vol. 34, 2018.

[31] R. Safari, R. Z. Amiri, and R. Esmaeilzadeh Kenari, "Antioxidant and antibacterial activities of C-phycocyanin from common name Spirulina platensis," Iran. J. Fish. Sci., vol. 19, no. 4, pp. 1911–1927, 2020.

[32] M. Kavisri, Marykutty Abraham, Gopal Prabakaran, Manickam Elangovan, and Meivelu Moovendhan, "Phytochemistry, bioactive potential and chemical characterization of metabolites from marine microalgae (Spirulina platensis) biomass," Biomass Convers. Biorefinery, no. 0123456789, 2021.

[33] R. Challouf et al., "Evaluation of cytotoxicity and biological activities in extracellular polysaccharides released by cyanobacterium Arthrospira platensis," Brazilian Arch. Biol. Technol., vol. 54, no. 4, 2011.

[34] J. Mofeed, M. Deyab, and E. El-Bilawy, "In vitro Anticancer Potentialities of Three Egyptian Cyanobacterial Isolates against Breast Adenocarcinoma and Hepatocellular Carcinoma Cell Lines," Egypt. J. Bot., vol. 62, no. 2, 2022.

[35] M. Maryati et al., "Cytotoxic effect of spirulina platensis extract and ulva compressa linn. On cancer cell lines," Food Res., vol. 4, no. 4, pp. 1018–1023, 2020.

[36] S. Deshpande, S. Sharma, V. Koul, and N. Singh, "Core-shell nanoparticles as an efficient, sustained, and triggered drug-delivery system," ACS Omega, vol. 2, no. 10, 2017.

[37] S. Deng, M. R. Gigliobianco, R. Censi, and P. Di Martino, "Polymeric nanocapsules as nanotechnological alternative for drug delivery system: Current status, challenges and opportunities," Nanomaterials, vol. 10, no. 5. 2020.

[38] L. Li, L. Lu, and C. Zhou, "Notice of Retraction: Fabrication of injectable PLLA/alginate hydrogel for tissue engineering," 5th International Conference on Bioinformatics and Biomedical Engineering, iCBBE 2011. 2011.

[39] A. Banerjee, J. Qi, R. Gogoi, J. Wong, and S. Mitragotri, "Role of nanoparticle size, shape and surface chemistry in oral drug delivery," J. Control. Release, vol. 238, 2016.

[40] M. Chopra, P. Kaur, M. Bernela, and R. Thakur, "Synthesis And Optimization of Streptomycin Loaded Chitosan-Alginate Nanoparticles," Int. J. Sci. Technol. Res., vol. 1, no. 10, pp. 31–34, 2012.

[41] S. Li et al., "Application of chitosan/alginate nanoparticle in oral drug delivery systems: prospects and challenges," Drug Deliv., vol. 29, no. 1, pp. 1142–1149, 2022.

[42] N. V. N. Jyothi, P. M. Prasanna, S. N. Sakarkar, K. S. Prabha, P. S. Ramaiah, and G. Y. Srawan, "Microencapsulation techniques, factors influencing encapsulation efficiency," J. Microencapsul., vol. 27, no. 3, pp. 187–197, 2010.

[43] L. Younis, M. Hassan, and T. Ali, "Periodontitis: A Cellular Tactic to Escape Cancer," Annu. Res. Rev. Biol., vol. 23, no. 6, 2018.

[44] M. A. Mohammed, J. T. M. Syeda, K. M. Wasan, and E. K. Wasan, "An overview of chitosan nanoparticles and its application in non-parenteral drug delivery," Pharmaceutics, vol. 9, no. 4, 2017.

[45] X. B. Yin, Q. Z. Yu, B. W. Li, and C. D. Zhang, "Preparation and Characterization of Sodium Alginate/Chitosan Composite Nanoparticles Loaded with Chondroitin Sulfate," Adv. Mater. Sci. Eng., vol. 2021, 2021.

[46] M. H. Kafshgari, M. Khorram, M. Mansouri, A. Samimi, and S. Osfouri, "Preparation of alginate and chitosan nanoparticles using a new reverse micellar system," Iran. Polym. J. (English Ed., vol. 21, no. 2, pp. 99–107, 2012.

[47] B. İnan, R. Çakır Koç, and D. Özçimen, "Comparison of the anticancer effect of microalgal oils and microalgal oil-loaded electrosprayed nanoparticles against PC-3, SHSY-5Y and AGS cell lines," Artif. Cells, Nanomedicine Biotechnol. vol. 49, no. 1, 2021.

[48] A. Bedini, L. Mercy, C. Schneider, P. Franken, and E. Lucic-Mercy, "Unraveling the initial plant hormone signaling, metabolic mechanisms and plant defense triggering the endomycorrhizal symbiosis behavior," Front. Plant Sci., vol. 871, no. December, pp. 1–28, 2018.

[49] N. W. S. Agustini and Y. Wijayanto, "Isolation, identification of fatty acids from Spirulina platensis as antibacterial," IOP Conf. Ser. Earth Environ. Sci., vol. 457, no. 1, 2020.

[50] M. Deyab, M. El-Sheekh, R. Hasan, A. Elsadany, and S. Abu Ahmed, "Phytochemical Components of Two Cyanobacterial Local Strains," Sci. J. Damietta Fac. Sci., vol. 11, no. 1, pp. 67–75, 2021.

[51] B. Cai, X. Zhao, L. Luo, P. Wan, H. Chen, and J. Pan, "Structural characterization, and in vitro immunostimulatory and antitumor activity of an acid polysaccharide from Spirulina platensis," Int. J. Biol. Macromol., vol. 196, 2022.